García Pérez, JV.; Ortuño Cases, C.; Puig Gómez, CA.; Carcel Carrión, JA.; Pérez Munuera, IM. (2012). Enhancement of Water Transport and Microstructural Changes Induced by High-Intesity Ultrasound Application on Orange Peel Drying. Food and Bioprocess Technology. 5:2256-2265. doi:10.1007/s11947-011-0645-0.

Enhancement of water transport and microstructural changes induced by high intensity ultrasound application on orange peel drying.

Jose V. Garcia-Perez[1*], Carmina Ortuño[1], Ana Puig[2], Juan A. Carcel[1], Isabel Perez-Munuera[2]

[1]Grupo de Análisis y Simulación de Procesos Agroalimentarios, Departamento Tecnología de Alimentos, Universidad Politécnica de Valencia, Camí de Vera s/n, E46022, Valencia, Spain, jogarpe4@tal.upv.es

[2]Grupo de Microestructura y Química de Alimentos, Departamento Tecnología de Alimentos, Universidad Politécnica de Valencia, Spain

Short running title: *Enhancement of orange peel drying by ultrasound*

*Corresponding author: J.V. Garcia-Perez (Teleph: +34963879376, Fax: +34963879839, e-mail: jogarpe4@tal.upv.es)

Abstract

The main aim of this work was to evaluate the effect of high intensity ultrasound on drying kinetics of orange peel as well as its influence on the microstructural changes induced during drying. Convective drying kinetics of orange peel slabs were carried out at 40 °C and 1 m/s with (AIR+US) and without (AIR) ultrasound application. Drying kinetics analysis was addressed by considering diffusion theory in order to identify the influence of ultrasound on water transport. Fresh, AIR and AIR+US dried samples were analyzed using Cryo-Scanning Electron Microscopy. Results showed that drying kinetics of orange peel were significantly improved by the ultrasonic application, which involved a significant ($p<0.05$) improvement of both mass transfer coefficient and effective moisture diffusivity. The effects on mass transfer properties were confirmed from microstructural observations. In the cuticle surface of flavedo, the pores were obstructed by the spread of the waxy components, this fact evidencing the ultrasonic effects on the interfaces. The cells of the albedo were degraded by application of ultrasound as it brought about large intercellular air spaces facilitating water transfer through the tissue.

Key words: dehydration, microstructure, modeling, ultrasonic.

Introduction

Orange production in the world reached an average of 63 millions of tons for the period 1997-2007 (FAOSTAT, 2010). Brazil and USA are the main producers, Spain gets the 5th position as world producer, with almost the half of the production of the European Union. The major part of the orange production in Spain is concentrated in the Mediterranean area, and especially in the Valencia region (Spanish Ministry of the Environment and Rural and Marine Affairs, 2009). In the world market, 40% of the orange production is used in orange juice processing, which generates an average mass of waste of 0.5 kg per kg of raw orange that may be considered an environmental issue in terms of disposal. Traditionally, orange juice waste has been used as animal feeding (Garau et al., 2006) providing an additional but low income for the orange industry. As a consequence, perspective studies are essential in order to search for new alternatives and as consequence, to increase the value of this by-product. Some orange peel components may present high interest due to their healthful properties. References may be found in the literature reporting the high antioxidant activity (Larrauri et al., 1996; Garau et al., 2007; Anagnostopoulou et al., 2006) and fiber content (Garau et al., 2007; Chau et al., 2005) of orange peel. In both applications, drying of raw matter is considered a preliminary and necessary step with great importance concerning not only in the terms of energy consumption but also the quality of the final product. Thus, Garau et al., (2006) reported that drying of orange peel is the most expensive step in dietary fiber production. As a consequence, exploratory studies about new drying technologies to be applied on drying may be considered subject of relevant research (Mujumdar & Law, 2010).

High intensity (or power) ultrasound application is considered an emergent technology to be applied in food processing, its use is already being common in applications in liquid media by using ultrasonic baths. Ultrasonic assisted hot air drying of foods has been showed highly efficient in order to increase the drying rate of several products, among others carrots (Gallego-Juárez et al., 1999; García-Pérez et al., 2006; Garcia-Perez et al., 2009), persimmon (Cárcel et al., 2007) and lemon peel (García-Pérez et al., 2006; García-Pérez et al., 2007). The effects that high intensity ultrasound produces over a target process depend on the physical structure of the medium in which waves are travelling. Thereby, ultrasound may be used to form aggregates on gas media or to separate it in liquids. The improvement on hot air drying rate is a consequence of the phenomena produced by ultrasound over the global mass transfer resistance. In one hand, ultrasound produce alternative expansions and contraction of the material (sponge effect) that facilitates water transfer through the sample until the surface. In the other hand, convective mass transfer may be enhanced by pressure variation, oscillating velocity and microstreaming that ultrasound produced on the solid-gas interfaces reducing boundary layer thickness (Gallego-Juarez, 1998). Previous works based on computational analysis of drying kinetics have confirmed the influence of ultrasound on both internal and external mass transfer resistance (García-Pérez et al., 2006 and 2009; Cárcel et al., 2007). The influence of high intensity ultrasound on drying rate depends on the magnitude of the process variables involved as well as the product's structure. As a consequence, in order to determine the influence of ultrasonic application on the drying of a target product it is necessary to analyze the drying kinetics.

The study of the influence that ultrasound produces on the microstructure can contribute to fully develop the ultrasonic assisted drying of foods. The analysis is essential not only to explain the influence of ultrasound on mass transfer process but also in terms of quality. Previous literature has already reported significant structural effects associated to ultrasonic application in food processing. Ultrasonically assisted salted cheeses presented a higher firmness after ripeness than conventional salted ones (Sanchez et al., 2001a; Sanchez et al., 2001b), which was explained by a more intense degradation of fatty acids and proteins. The application of power ultrasound during red pepper salting process involved a high cell degradation, which produced a reduction of the firmness (Gabaldon-Leyva et al., 2007). Toma et al. (2001) identified, using a light microscope, a very intense degradation of oil glands in mint leaves during ultrasonic assisted extraction. The application of ultrasound like a pretreatment prior to oil extraction (Sharma & Gupta, 2006) and air drying process (Fernandes et al., 2008a; Fernandes et al., 2008b; Oliveira et al., 2010) has also involved effects on the product structure, which has promoted the subsequent mass transfer processes. The entire works are addressing ultrasonic applications in solid-liquid media but, as far as we know, references addressing the influence of ultrasonic assisted air drying on product's microstructure have not been reported in previous literature. Microstructure analysis is widely spread in literature to describe structural changes in foods during postharvest or processing (Chafer et al., 2003; Salvador et al., 2008; Alandes et al., 2009; Cruz et al., 2010).

The main aim of this work was to determine the influence of high intensity ultrasound application on orange peel drying, relating the water transport

phenomena with the structural changes induced during the process. In order to reach this objective, computational and microstructure analysis were considered necessary tools.

Materials and methods

Raw materials

Fresh orange fruits (*Citrus sinensis* var. Navelina) were picked in Gata (Alicante, Spain) in an advanced stage of ripeness. The whole pieces were washed, strained and stored at 4±1ºC until processing. The orange peel was separated from the flesh by hand and cut into parallelepipeds (height 80.0±2.5 mm, width 40±2.0 mm, thickness 5.9 ± 0.4 mm). Samples were wrapped in plastic films to avoid moisture loss, and maintained at 4°C until processing. In any case, storage time was always shorter than 24 h.

The initial moisture content of the orange peel was 2.89 ± 0.14 (kg water/kg dry matter), according to AOAC method 934.06 (AOAC, 1997). The measurement was carried out in triplicate at 70ºC and 800 mbar vacuum levels until constant weight (24 ±1 h).

Drying experiments

Drying kinetics were carried out in a high intensity ultrasonic assisted convective drier already described in previous works (Fig. 1) (García-Pérez et al., 2006, Cárcel et al., 2007). An air borne ultrasonic device constitutes the drying chamber, it includes an aluminum vibrating cylinder (internal diameter 10 cm, height 31cm and thickness 1cm) driven by a piezoelectric composite

transducer (21.7 kHz). The ultrasonic device is able to generate a high-intensity ultrasonic field in the medium (154.3 dB). The drier operates in automatic mode; air temperature and velocity are controlled and a balance is used to weight the samples at preset times.

Air drying experiments (AIR) of orange peel slabs were carried out at constant air velocity and temperature, 1 m/s and 40ºC, respectively. Drying experiments assisted by high intensity ultrasound (AIR + US) were carried out at the same experimental conditions than AIR experiments and by applying the electric powers of 90 and 45 W to the ultrasonic transducer. In all the cases, drying experiments were conducted in triplicate and completed when samples lost 70% of the initial weight. Drying kinetic was determined from the initial moisture content and the weight loss logged during drying.

The total energy consumption during drying experiments was measured using a digital power meter (FLUKE 430, Fluke Ibérica, Madrid, Spain). The main elements to be considered in the quantification of the energy consumption were the heating elements, the ventilation system (fan) and the ultrasonic power generator.

Cryo-Scanning Electron Microscopy (Cryo-SEM)

The microstructure of fresh-cut, AIR and AIR+US dried samples was studied using Cryo-SEM (Salvador et al., 2008). In all the cases, the analysis was carried out in both sample's surface and sections. The experimental set-up involves a Cryostage CT-1500C (Oxford Instruments, Witney, UK) coupled to a Jeol JSM-5410 scanning electron microscope (Jeol, Tokyo, Japan). Samples

were immersed in slush N_2 (at -210 ºC) and then quickly transferred to the Cryostage at 1 kPa, where sample fracture took place. The sublimation was carried out at -95 ºC and the final point was determined by direct observation in the microscope (5 kV). Once again in the Cryostage unit, the sample was coated with gold using an ionization current of 2 mA and applying vacuum (0.2 kPa) for 3 min. The observation in the scanning electron microscope was carried out at 15 kV, a working distance of 15 mm and -130 ºC.

Computational analysis of drying kinetics

Drying kinetics were mathematically described using a diffusion model (Ruiz-Lopez et al., 2010) assuming orange peel parallelepipeds behave as infinite slab geometry (Garau et al., 2006) because two dimensions are larger compared to the third one (thickness). The mass flow on the thickness direction being much larger compared to the other ones due to the relative mass transfer resistances (Perry & Chilton, 1973; Singh & Heldman, 2001). The governing equation (Eq. 1) was solved by considering the orange peel as homogeneous and isotropic material, the initial moisture content and temperature uniform and the effective moisture diffusivity and sample volume constant during drying (García-Pérez et al., 2007).

$$\frac{\partial W_p(x,t)}{\partial t} = D_e\left(\frac{\partial^2 W_p(x,t)}{\partial x^2}\right) \quad (1)$$

Where W_p is the local moisture content (d.b., kg water/kg dry matter), D_e is the average effective moisture diffusivity (m^2/s), t is the time (s) and x is the characteristic direction of the water transport.

The governing equation was solved considering two different approaches. First, the external resistance was neglected (NER model) assuming that drying depends only on internal water transport through the solid and that the product surface is maintained in equilibrium with air drying (Eq. 2).

$$t > 0 \qquad x = L \qquad \tau(L,t) = W_e \tag{2}$$

Orange cuticle is covered by waxy compounds (Chafer et al., 2003), thus, it was considered as a waterproof layer, being the characteristic dimension for water transport (L), the total thickness of orange peel slabs. Equilibrium data for drying of orange peel were obtained from literature (Garau et al., 2006).

The solution of the NER model is depicted in Eq. 3 in terms of the average moisture content (Crank, 1975; Simal et al., 1998) (Eq. 3).

$$W(t) = W_e + (W_c - W_e) \sum_{n=0}^{\infty} \frac{8}{(2n+1)^2 \pi^2} \exp\left(\frac{-D_e (2n+1)^2 \pi^2 t}{4L^2} \right) \tag{3}$$

In the NER model, the effect of the external resistance on mass transfer is included in the effective diffusivity, this being a fitting parameter including both diffusion kinetics mechanisms, and other kinetic effects do not considered in the NER model.

As second approach for modeling, the external resistance to mass transfer was considered in the diffusion model (ER model) in terms of kinetic control. The ER model provides the joint evaluation of the influence of high intensity ultrasound on both external and internal resistance to mass transfer by means of the quantification of the effective moisture diffusivity and the mass transfer coefficient.

The ER model was solved by considering the water flux equality between solid surface and air (Eq. 4) (Guiné et al., 2010).

$$- D_e \rho_{ds} \frac{\partial W_p(L,t)}{\partial x} = k\left(\varphi_e(L,t) - \varphi_{air}\right) \quad (4)$$

Where ρ_{ds} is the dry solid density (kg/m^3), k is the mass transfer coefficient (kg w/m^2/s) which determines the water transfer rate from the solid surface to the air medium, φ_e is the air relative humidity of the air at equilibrium with the surface of the material ($x=L$) and φ_{air} is the relative humidity of the hot air. The dry solid density was determined by liquid displacement using toluene, a volumetric standard picnometer of 48.889 mL and an analytical balance (±0.001 g, PB 303-S, Mettler Toledo).

The ER model was applied by using an implicit finite difference method (Mulet et al., 2005) to solve the diffusion equation assuming the boundary condition stated in Eq. 4. The solid volume was divided in a finite number of subvolumes characterized by its node (central point). Eq. 5 shows the general relationship of the local moisture content for a node, being a function of the moisture content both of the neighbor nodes and of the same node at a previous time. The particular expression at each kind of node must be obtained by adequately combining the boundary conditions (Simal et al., 2003).

$$\tau(i,t-\Delta t) = \frac{D_e \Delta t}{\Delta x^2}\left[\tau(i,t)\left(\left(\frac{\Delta x^2}{D_e \Delta t}\right)+2\right) - \tau(i+1,t) - \tau(i-1,t)\right] \quad (5)$$

The position of the node is characterized by the x coordinate, the separation between nodes by $\Delta x=L/(n-1)$, the number of nodes by n=15 and, finally, the

time interval considered by Δt.

The implicit equations system obtained for the node net was solved by programming a series of functions in Matlab (Matlab® 7.1 SP3, The MathWorks, Inc., Natick, MA, USA). Thus, the moisture profile in an infinite slab geometry body may be obtained as a function of the thickness, the effective diffusivity and the mass transfer coefficient. The calculation by integration of the average moisture content of the solid was also implemented in the Matlab code.

Kinetic parameters estimation (D_e in NER; D_e and k in ER models) was carried out by an unconstrained nonlinear optimization method (Simplex). Identification was performed by minimizing the sum of the squared differences between the experimental and the calculated average moisture content considering kinetic parameters as predictor variables. In the case of the ER model, for the parameters D_e and k the joint interval of confidence (95% statistical significance) was calculated in order to estimate the consistency of the simultaneous identification. A sub-function was programmed in Matlab code to include the iterative calculation in the solution of the diffusion model.

The fit of the model to the experimental data was computed by assessing the explained variance (VAR, Eq. 6).

$$VAR = \left\lfloor 1 - \frac{S^2_{tW}}{S^2_W} \right\rfloor \times 100 \qquad (6)$$

where S^2_W and S^2_{tW} are the variance of the sample and the estimation, respectively.

Analysis of variance (ANOVA) and LSD intervals ($p<0.05$) were carried out

using Statgraphics Plus 5.1. (Statistical Graphics Corp.) to estimate significant statistical differences in D_e and k produced by high intensity ultrasound application.

Results and Discussion

Experimental drying data

Orange peel presented an average initial moisture content of 2.89±0.14 (kg water/kg dry matter), which was considered the critical moisture content due to the constant rate period was not observed during experimentation. Fig. 2 shows experimental drying kinetics of orange peel slabs carried out without (AIR) and with high intensity ultrasound application (AIR+US), at the two different ultrasonic powers tested, 45W (AIR+US-45W) and 90W (AIR+US-90W).

Dry samples presented a final moisture content of 0.12±0.05 (kg water/kg dry matter), which corresponds with a weight loss of 70% for the raw orange peel. In order to reach the final moisture content, AIR drying experiments were extended until an average drying time of 9.7 hours. The application of high intensity ultrasound reduced the drying time at approximately 6.9 hours for AIR+US-45W and at 5 hours for AIR+US-90W, meaning a reduction of drying time of 30 and 45%, respectively. This fact suggests an improvement of water removal rate during drying by ultrasonic application, and obviously, the effect has been dependent on the applied ultrasonic power. The influence of high intensity ultrasound has already been showed for other agri-food products, like lemon peel (García-Pérez et al., 2007), carrot (Gallego-Juarez et al., 1999; García-Pérez et al., 2006 and 2007) and persimmon (Cárcel et al., 2007;

García-Pérez et al., 2007). The reduction of drying time also resulted in energy saving, which was evaluated by measuring the total energy consumption using a digital power meter. Thus, the total energy used during drying was reduced in 12 and 20% for AIR+US-45W and AIR+US-90W experiments regarding AIR experiments, respectively. As it was already mentioned, drying is considered a highly demanded energy operation; therefore, the ultrasonic application may involve a significant improvement of drying process in terms of energy consumption.

A simple analysis of drying kinetics does not provide more information about the effect of high intensity ultrasound on mass transfer phenomena. Modeling is considered a fundamental tool to explain and clarify the origin of drying improvement by high intensity ultrasound. In addition, a deep knowledge of mass transfer phenomena would be essential to correlate with microstructure analysis.

Influence of high intensity ultrasound on mass transfer transport

The results of drying kinetics modeling are shown in Table 1 for NER and ER diffusion models. Effective moisture diffusivity, identified by fitting the NER model to experimental data, increased significantly from 0.88×10^{-9} to 1.33×10^{-9} m^2/s by applying an ultrasonic power of 45W during drying experiments. The improvement was even higher when the applied power reached 90W (1.72×10^{-9} m^2/s). This result involves a significant ($p<0.05$) improvement of internal water transport by ultrasonic application, being dependent the effect on the applied ultrasonic power. Literature has already reported this fact for other foodstuffs

(Gallego-Juarez et al., 1999; Cárcel et al., 2007; García-Pérez et al., 2007 and 2009), linking the ultrasonic effect on the internal mass transport to the alternative expansions and compressions produced in the material by the ultrasonic wave. This effect is reported as “sponge effect” due to its similarity when a sponge is squeezed and released (Gallego-Juarez, 1998).

The NER diffusion model led to a poor fit of drying kinetics, explained variance reached was lower than 95.5% in all the cases (Table 1). Fig. 3 contributes to illustrate, for a particular case, the lack of agreement between experimental and calculated data from NER model. These results points to the fact that assumptions considered in NER model deviate from the real behavior occurring in orange peel drying. Thus, the effective moisture diffusivity showed in Table 1 includes not only the phenomena linked to diffusion but also those mechanism unknown and not considered in modeling. Therefore, the effective moisture diffusivity must be considered a simple kinetic fitting parameter. However, the diffusivity identified from NER model results useful to address more complex models, like the ER model, due to it is used as initial value in the optimization problem to fit the new model to the experimental drying kinetics.

The ER model provided a better fit of experimental data and higher agreement between experimental drying and calculated data was found using ER model than using NER model (Fig. 3). The goodness of the fit of the ER model is illustrated by the explained variance reached, which was higher than 99% in all the cases. This result suggests that in order to describe adequately mass transport during orange peel drying, the external resistance to mass transfer must be considered a significant effect. The low air velocity used in drying experiments, 1 m/s, makes un-negligible the water transport resistance from

solid surface to air medium, which has been already confirmed by literature data (Carcel et al., 2007). In addition, the use of ER model permits to separate the influence of high intensity ultrasound on both internal and external resistance to mass transfer, by quantifying not only the effective moisture diffusivity (D_e) but also the mass transfer coefficient (k) (Table 1).

Effective moisture diffusivity identified using the ER model followed the same trend than in the NER model. The application of high intensity ultrasound resulted in the increase of the effective moisture diffusivity and the improvement was higher applying 90 than 45W. Higher ultrasonic powers than 90W could not be reached due to safety requirements in the ultrasonic set-up. Therefore, the aforementioned effects of high intensity ultrasound application on internal mass transfer were confirmed by using the ER model.

A significant ($p<0.05$) effect of power ultrasound on mass transfer coefficient (k) was also identified (Table 1). Thus, the k values identified increased by 45% if AIR experiments are compared to AIR+US-45W, the improvement was even larger when an ultrasonic power of 90W was applied (AIR+US-90W). This results show a significant reduction of external resistance to mass transfer by the ultrasonic application, which may be explained by the shaking effect on the interfaces associated to the ultrasonic waves (Gallego-Juarez et al., 1999; García-Pérez et al., 2007). Ultrasound waves produce pressure variations, oscillating velocities and micro-streamings creating a high turbulence around the particle (shaking effect) and reducing the thickness of the boundary layer, which results in the increase of the mass transfer coefficient.

The proper modeling of the drying kinetics using the diffusion model considering

external resistance to mass transfer (ER model) allowed not only to quantify the effect of ultrasound on water transport but also to separate it between external and internal transport mechanisms.

Influence of high intensity ultrasound on microstructure

The effects associated to ultrasonic application on mass transfer may be analyzed by addressing the influence of ultrasonic application on microstructure of dried orange peel, trying to establish links between the ultrasonic effect on water transfer and microstructure changes.

As it is well known, two main tissues are considered in orange peel, flavedo and albedo. Flavedo constitutes the external layer of orange peel and albedo is the internal one. The first step of the study must be the microstructural characterization of the fresh orange peel, since it has not been yet reported in literature.

Flavedo is covered by a waxy and thin layer, named cuticle (Fig. 4A), which protects the orange fruit from dehydration and other external agents during growing. The microstructural study reveals the existence of pores in the cuticle. These pores (25-30 μm) are ring-shaped and they are surrounded by waxy accumulations (Fig. 4A). The cuticle is closely connected with the flavedo cells (Fig. 4B). The main components of the flavedo are spherical or oval cells without practically intercellular spaces (Fig. 4B and 4C). The typical eutectic artifact can be observed in these cells (Fig. 4D), which is generated by the etching process during the preparation of the samples. The structure of this artifact is similar to a very close network, which indicates that there is a large

quantity of soluble solids inside these cells, situated mainly in the vacuole (Fig. 4D)

In the fresh orange samples, the albedo tissue is constituted by interconnected tubular cells with large intercellular spaces among them (Fig. 5A). Continuity is observed between flavedo and albedo tissues, as it goes into the internal layers, larger intercellular spaces, occupied by air, and the tubular cells of the albedo tissue can be observed (Fig. 5B and 5C). Inside these cells, the typical eutectic artifact denser than in the flavedo cells was also found (Fig. 5D), which could indicate a higher concentration of solutes in the albedo cells.

Air drying treatment produces the shrinkage of the orange peel, which is considered a usual phenomenon in drying processes (Khalloufi et al., 2009). As can be observed in Fig. 6, there is a higher quantity of pores by area in the AIR dried (Fig. 6B) than in the fresh sample (Fig. 6A), which reveals shrinkage during drying. This effect was also shown in the section of the orange peel (Fig. 7). In the fresh sample (Fig. 7A), cuticle and only the first cell layers of the flavedo are observed. However, when these samples are dried (AIR+US-90 W) both tissues (flavedo and albedo) can be observed in the same area (Fig. 7B). Both images have been selected at the same magnification, thus the observed differences may be also attributed to the shrinkage experimented by orange peel during drying. From microstructural analysis, a similar shrinkage pattern was found when AIR and AIR+US dried samples are compared.

Air drying provoked the loss of the characteristic distribution of the waxy components on the peel surface. The waxy components spread on the cuticle surface resulting in the obstruction of some pores (Fig. 6C). The spread of the

waxy components generated a waterproof barrier, and as a consequence, water transfer through this surface must be more difficult during the air drying process. This fact suggests that water movement is facilitated to be occurred mainly through albedo, which was also taking in the modeling into account by considering the characteristic dimension (L) for the diffusion the total thickness of the orange peel (5.9 mm).

Despite the spread of the waxy component in the air dried samples (AIR) (Fig. 6C), the ring shape around the pores is still well defined. However, after the ultrasound application (AIR+US-90W), the typical ring-shape around the pores appears blurred (Fig. 6D) and all the pores are completely obstructed. The application of high intensity ultrasound involves a more intense spread of the waxy compounds on the cuticle surface. The intense spread of waxy compounds observed on the cuticle confirms effects on the interfaces promoted by ultrasonic application. The aforementioned mechanical effects (shaking) produced by ultrasonic waves on the interfaces should bring about not only a greater spread of waxy components on the cuticle but also the improvement of water transfer from the surface of the albedo (situated on the opposite side of the cuticle surface). Both cuticle and albedo surfaces are considered interfaces in the orange peel slabs, obviously, it must be remarked that depending on the characteristics of the interfaces involved, the effects produced by ultrasound in the interfaces will be different (Gallego-Juárez et al., 1999).

In the case of the inner structure of the albedo, the fresh cellular tissue (Fig. 8A) is disrupted by air drying (AIR) (Fig. 8B) disappearing the cell tubular shape due to the water removal. It is well known that the water release during drying process brings about a high stress on the vegetable cells, which results in a

collapse of the typical cell structure. The application of high intensity ultrasound (AIR+US-90W) (Fig. 8C) produced even a more intense disruption of the albedo cells than in AIR dried samples (Fig. 8B). The cellular structure is highly degraded and large intercellular spaces can be observed after drying. The alternative expansions and compressions produced by ultrasonic waves (sponge effect) in the material contribute to the more intense cellular tissue degradation. The acoustic wave acts repeatedly over the cell facilitating water release as well as, affecting cellular structure. Therefore, the microstructural analysis revealed an effect of power ultrasound on the internal structure of the orange peel, which confirms the significant effect of ultrasonic application over internal water transport identified from modeling.

Conclusions

The application of high intensity ultrasound reduced the drying time of orange peel. The effect was more intense as the applied ultrasonic power increased. A time reduction may be associated to energy and economic saving at industrial scale.

From modeling, the ultrasonic effect on drying kinetics was well explained from a significant ($p<0.05$) improvement of the effective moisture diffusivity and the mass transfer coefficient. That fact suggests an influence of ultrasonic application on both internal and external water transport.

The results about the ultrasonic influence on water transport during drying were confirmed and explained from microstructural analysis. An ultrasonic effect on interfaces was observed resulting in a more intense spread of waxy compounds

on the cuticle surface, which may be correlated to the improvement of water transport between albedo surface and air medium. In the internal structure of the orange peel, ultrasound produced a higher degradation of albedo tissue by alternative expansions and contraction produced by ultrasonic wave, which also explains the improvement of water diffusion observed from modeling.

Acknowledgments

The authors would like to acknowledge the financial support of MICINN project Ref. DPI2009-14549-C04-04 and the European Union project FP6-2004-FOOD-23140 HIGHQ RTE.

References

Alandes, L., Perez-Munuera, I., Llorca, E., Quiles, A. & Hernando, I. (2009). Use of calcium lactate to improve structure of “Flor de Invierno” fresh-cut pears. Postharvest Biology and Technology. 53(3), 145-151.

Anagnostopoulou, M. A., Kefalas, P., Papageorgiou, V. P., Assimopoulou, A. N. & Boskou, D. (2006). Radical scavenging activity of various extracts and fractions of sweet orange peel (*Citrus sinensis*). Food Chemistry, 94(1), 19-25.

AOAC, (1997). Official methods of analysis. Association of Official Analytical Chemist, Arlington, Virginia, USA.

Cárcel, J. A., García-Pérez, J. V., Riera, E. & Mulet, A. (2007). Influence of high intensity ultrasound on drying kinetics of persimmon. Drying Technology, 25(1), 185-193.

Chafer, M., Gonzalez-Martinez, C., Chiralt, A. & Fito, P. (2003). Microstructure and vacuum impregnation response of citrus peles. Food Research International, 36(1), 35-41.

Chau, C., Sheu, F., Huang, Y. & Su, L. (2005). Improvement in intestinal function and health by the peel fibre derived from *Citrus sinensis* L cv Liucheng. Journal of the Science of Food & Agriculture, 85(7), 1211-1216.

Crank J. (1975). *The Mathematics of diffusion*. Oxford (2nd ed.), UK: Clarendon Press.

Cruz, R. M. S., Vieira, M. C., Fonseca, S. C., Silva, C. L. M. (2010). Impact of thermal blanching and thermosonication treatments on watercress

(*Nasturtium officinale*) quality: thermosonication process optimization and microstructure evaluation. Food and Bioprocess Technology, in press, DOI 10.1007/s11947-009-0220-0.

FAOSTAT (2010). FAO Statistical Databases. Food and Agriculture of the United Nations. Available at: http://faostat.fao.org/site/291/default.aspx. Accessed 15 January 2010.

Fernandes, F. A. N., Gallao, M. I. & Rodrigues, S. (2008a). Effect of osmotic dehydration and ultrasound pre-treatment on cell structure: Melon dehydration. Food Science and Technology, 41(4), 604-610.

Fernandes, F. A. N., Oliveira, F.I.P. & Rodrigues, S. (2008b). Use of ultrasound for dehydration of papayas. Food and Bioprocess Technology, 1(4), 339-345.

Gabaldon-Leyva, C. A., Quintero-Ramos, A., Barnard, J., Balandrán-Quintana, R., Talamás-Abbud, R. & Jiménez-Castro, J. (2007). Effect of ultrasound on the mass transfer and physical changes in brine bell pepper at different temperatures. *Journal of Food Engineering*, 81(2), 374-379.

Gallego-Juárez, J. A. 1998. Some applications of air-borne power ultrasound to food processing. In Povey, M.J.W.; Mason, T.J.*, Ultrasound in Food Processing*. UK: London, Chapman & Hall.

Gallego-Juárez, J. A., Rodríguez-Corral, G., Gálvez-Moraleda, J. C. & Yang, T. S. (1999). A new high intensity ultrasonic technology for food dehydration. Drying Technology, 17(3), 597-608.

Garau, M. C., Simal, S., Femenia, A. & Rosselló, C. (2006). Drying of orange skin: drying kinetics modelling and functional properties. Journal of Food Engineering, 75(2), 288-295.

Garau, M.C., Simal, S., Rossello, C. & Femenia, A. (2007). Effect of air-drying temperature on physico-chemical properties of dietary fibre and antioxidant capacity of orange (*Citrus aurantium* v. Canoneta) by-products. Food Chemistry, 104(3), 1014-1024.

García-Pérez, J.V., Cárcel, J.A., De la Fuente, S. & Riera, E. (2006). Ultrasonic drying of foodstuff in a fluidized bed. Parametric study. Ultrasonics, 44, 539-543.

García-Pérez, J.V., Cárcel, J.A., Benedito, J. & Mulet, A. (2007). Power ultrasound mass transfer enhancement in food drying. Food and Bioproducts Proccessing, 85(3), 247-254.

Guiné, R.P.F., Henrriques, F. & Barroca, M.J. (2010). Mass transfer coefficients for the drying of pumpkin (*Cucurbita moschata*) and dried product quality. Food and Bioprocess Technology, in press, DOI 10.1007/s11947-009-0275.

Khalloufi, S., Almeida-Rivera, C. & Bongers, P. (2009). A theoretical model and its experimental validation to predict the porosity as a function of shrinkage and collapse phenomena during drying. Food Research International, 42(8), 1122-1130.

Larrauri, J. A., Rupérez, P., Bravo, L. & Saura-Calixto, F. (1996). High dietary fibre powders from orange and lime peels: associated polyphenols and antioxidant capacity. Food Research International, 29(8), 757-762.

Mulet, A., Blasco, M., García-Reverter, J. & García-Pérez, J. V. (2005). Drying kinetics of *Curcuma longa* rhizomes. Journal of Food Science, 7(5), 318-323.

Mujumdar, A.S. & Law, C.L. (2010). Drying Technology: Trends and applications in postharvest processing. Food and Bioprocess Technology, in press, DOI 10.1007/s11947-010-0353-1.

Oliveira, F.I.P., Gallao, M.I., Rodrigues, S., Fernandes, F.A.N. (2010). Dehydration of malay Apple (*Syzygium malaccense* L.) using ultrasound as a pretreatment. Food and Bioprocess Technology, in press, DOI 10.1007/s11947-010-0351-3.

Perry, R.H. & Chilton, C.H. (1973). *Chemical Engineers' Handbook*. McGraw Hill (5^{th} ed.), New York, US.

Ruiz-López, I. I., Castillo-Zamudio, R. I., Salgado-Cervantes, M. A., Rodríguez-Jimenes, G. C., García-Alvarado, M. A. (2010). Mass transfer modelling during osmotic dehydration of hexahedral pineapple slices in limited volume solutions. Food and Bioprocess Technology, 3(3), 427-433.

Salvador, A., Salvador, L., Besada, C., Larrea, V., Hernando, I. & Perez-Munuera, I. (2008). Reduced effectiveness of the treatment for removing astringency in persimmon fruit when stored at 15°C: Physiological and microstructural study. Postharvest Biology and Technology, 49(3), 340-347.

Singh, R. P. & Heldman, D.R. (2001). *Introduction to Food Engineering*. Academic Press (3^{rd} ed.). San Diego, US.

Sanchez, E. S., Simal, S., Femenía, A., Benedito, J. & Roselló, C. (2001a). Effect of acoustic brining on lipolysis and on sensory characteristics of Mahon cheese. Journal of Food Science, 66(6), 892-896.

Sanchez, E. S., Simal, S., Femenía, A., Llul, P. & Roselló, C. (2001b). Proteolysis of Mahon cheese as affected by acoustic-assited brining. European Food Research and Technology, 212(2), 147-152.

Sharma, A. & Gupta, M. N. (2006). Ultrasonic pre-irradiation effect upon aqueous enzymatic oil extraction from almond and apricot seeds. Ultrasonics Sonochemistry, 13(6), 529-534.

Simal, S., Femenia, A. & Garcia-Pascual, P. (2003). Simulation of the drying curves of a meat-based product: effect of the external resistance to mass transfer. Journal of Food Engineering, 58(2), 193-199.

Simal, S., Rosello, C. & Mulet, A. (1998). Modelling of air drying in regular shaped bodies. Trends in Chemical Engineering, 4(4), 171-180.

Spanish Ministry of the Environment and Rural and Marine Affairs (2010). Agriculture Statistics. Available at: http://www.mapa.es/en/estadistica/infoestad.html. Accesed 20 January 2010).

Toma, M., Vinatoru, M., Paniwnyk, L. & Mason, T. J. (2001). Investigation of the effects of ultrasound on vegetal tissues during solvent extraction. Ultrasonics Sonochemistry, 8(2), 137-142.

Figure Captions.

Figure 1. Diagram of the ultrasonic assisted hot air drier.

Figure 2. Experimental drying kinetics of orange peel carried out at 40ºC and 1 m/s. Average value ± standard deviation (3 replicates).

Figure 3. Modeling of ultrasonic assisted drying kinetics (AIR+US-45W) of orange peel at 40 ºC and 1 m/s.

Figure 4. Cryo-SEM micrographs of flavedo cells from fresh orange peel: A) Surface of the cuticle covered by waxy material; B) Cuticle and flavedo cells; C) Detail of flavedo cells; D) Eutectic artifact inside of a flavedo cell. (P: pores; F: flavedo; C: cuticle; T: tonoplast (vacuole membrane); PM: plasmalem).

Figure 5. Cryo-SEM micrographs of albedo cells from fresh orange peel: A and B) Albedo cells showing a typical tubular structure; C) Albedo cells with large intercellular spaces occupied by air; D) Detail of an albedo cell. (IS: Intercellular spaces; EA: Eutectic artifact inside albedo cell).

Figure 6. Cryo-SEM micrographs of cuticle surface: A) Fresh orange peel; B) Air dried (AIR); C) Detail of pore in air dried (AIR); and D) Detail of pore in ultrasonic assisted dried (AIR+US-90W). (P: pores).

Figure 7. Cryo-SEM micrographs of cross sections from orange peel: A) Fresh; B) Ultrasonic assisted dried (AIR+US-90W). (F: flavedo; C: cuticle; A: albedo).

Figure 8. Cryo-SEM micrographs of albedo cells from orange peel. A) Fresh; B) Air dried (AIR); Ultrasonic assisted dried (AIR+US-90W).

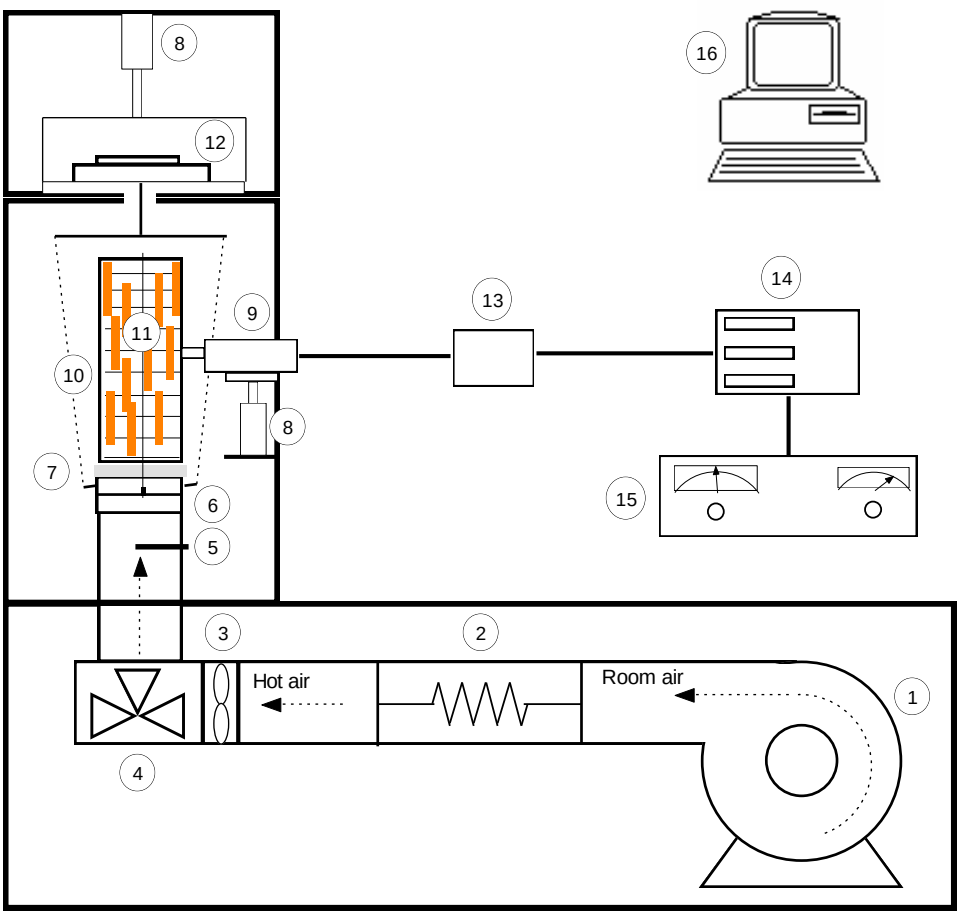

1. Fan, 2. Heating unit, 3. Anemometer, 4. 3-Way valve, 5. Thermocouple, 6. Sample loading chamber, 7. Coupling material, 8. Pneumatic moving arms, 9. Ultrasonic transducer, 10. Vibrating cylinder, 11. Sample loading tree, 12. Balance, 13. Impedance matching unit, 14. Watimeter, 15. High power ultrasonic generator, 16. PC

Figure 1

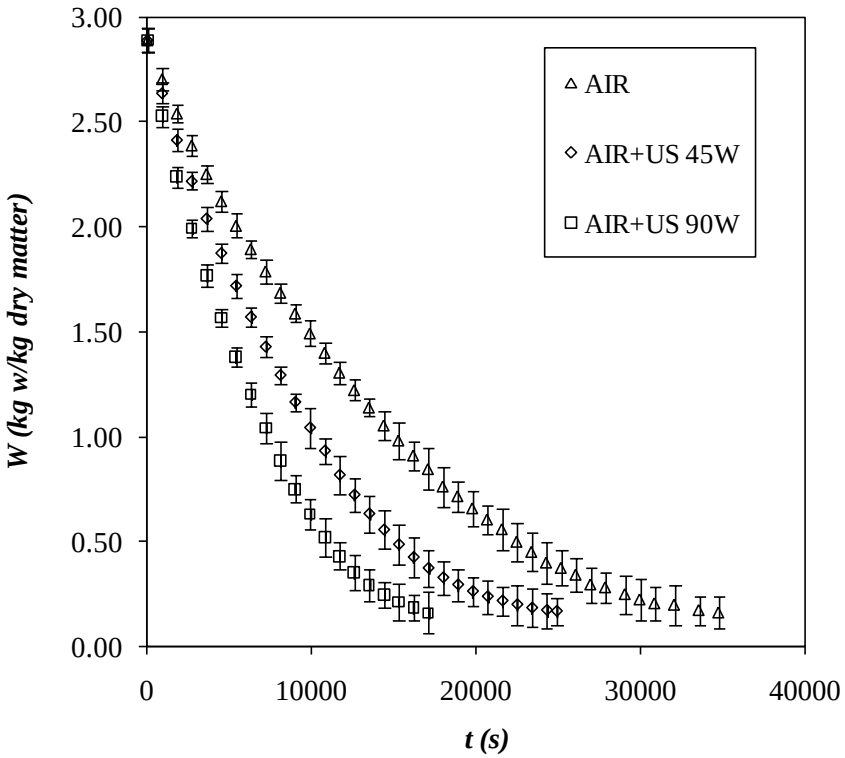
3.00
2.50
2.00
1.50
1.00
0.50
0.00
W (kg w/kg dry matter)
0
10000
20000
30000
40000
t (s)
AIR
AIR+US 45W
AIR+US 90W

Figure 2

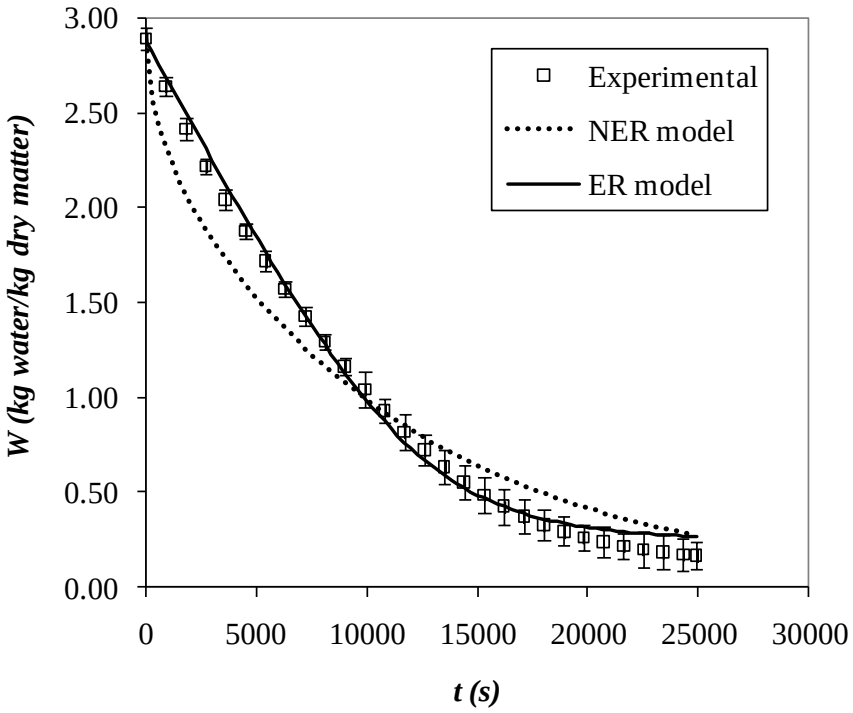
3.00
2.50
2.00
1.50
1.00
0.50
0.00
W (kg water/kg dry matter)
0
5000
10000
15000
20000
25000
30000
t (s)
Experimental
NER model
ER model

Figure 3

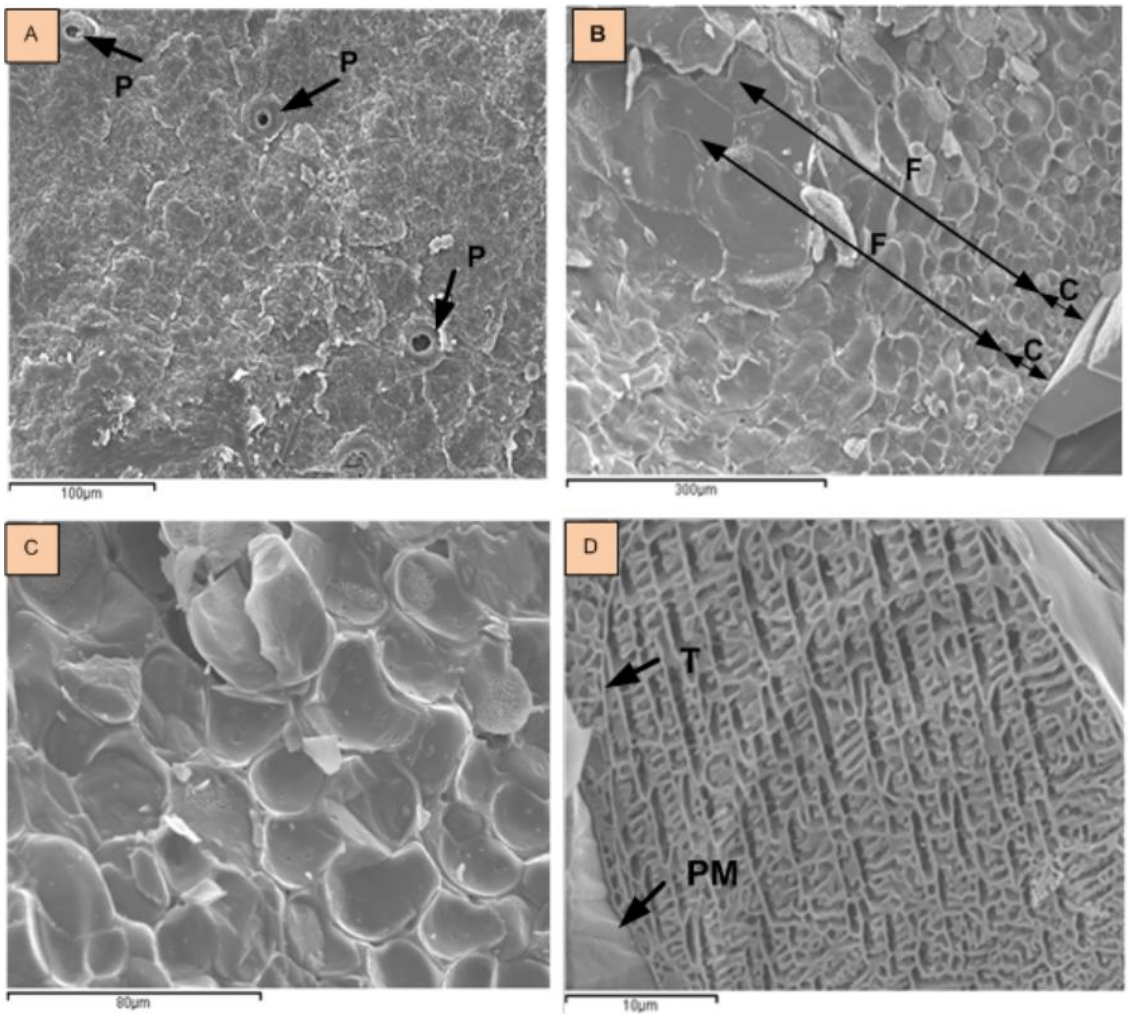

Figure 4

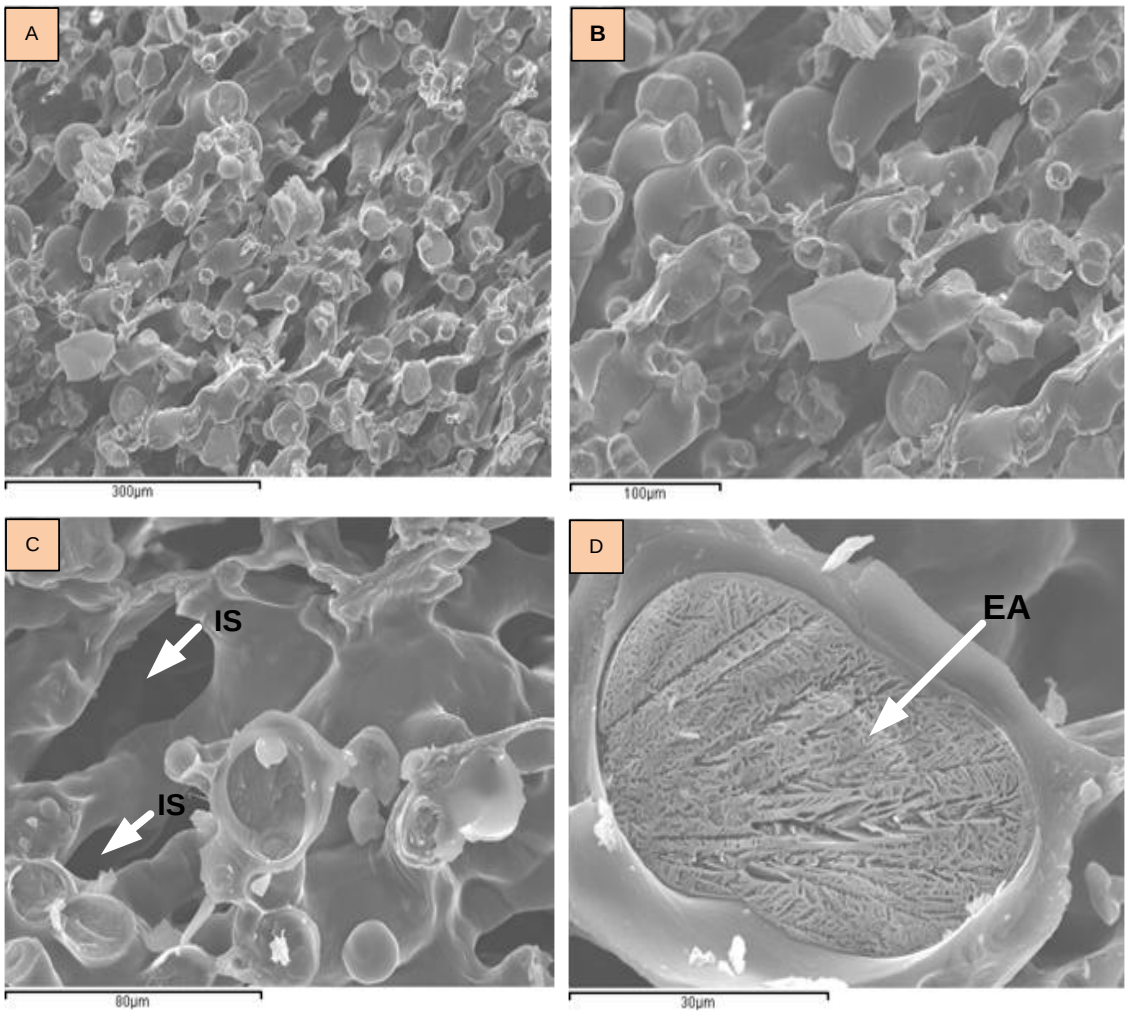

Figure 5

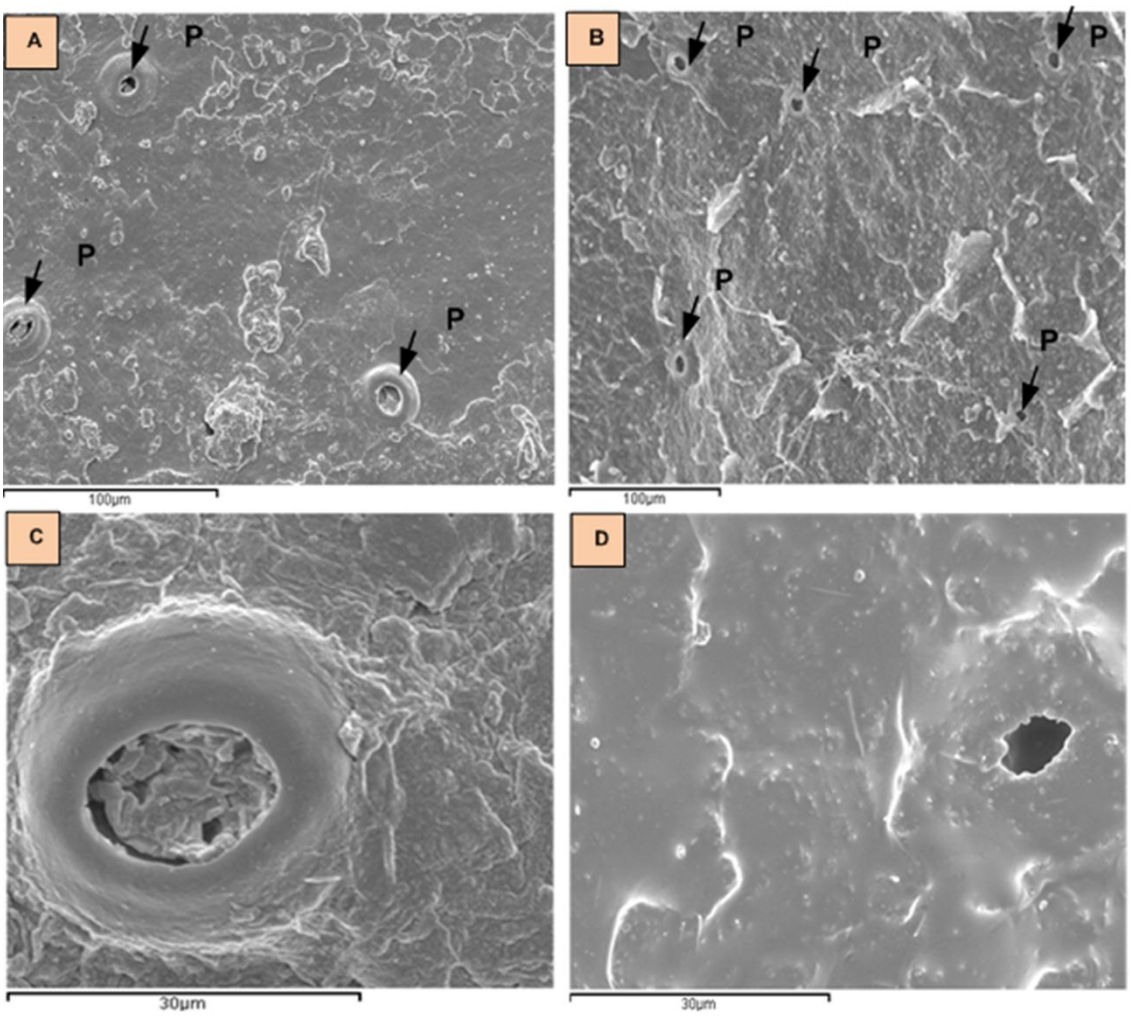

Figure 6

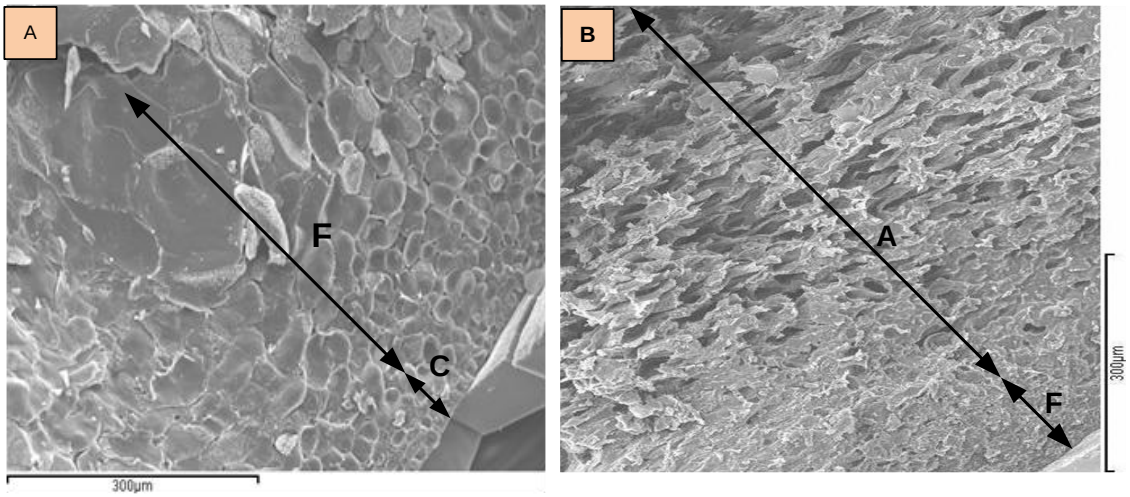

Figure 7

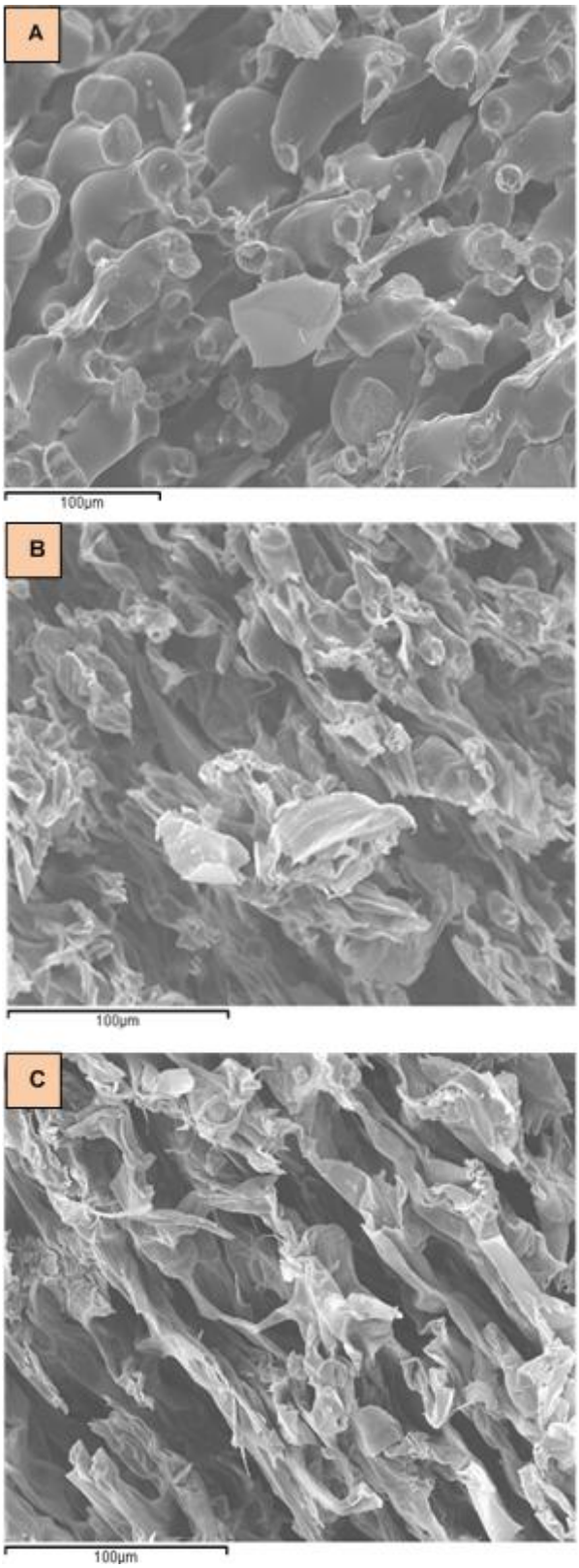

Figure 8

	NER model		ER model		
	D_e (10^{-9} m^2/s)	VAR (%)	D_e (10^{-9} m^2/s)	k (10^{-3} kg water/m^2/s)	VAR (%)
AIR	$0.88\pm0.06_A$	93.9	$4.04\pm0.44_D$	$1.17\pm0.05_X$	99.3
AIR+US-45W	$1.33\pm0.08_B$	94.1	$5.65\pm0.72_E$	$1.72\pm0.04_Y$	99.3
AIR+US-90W	$1.72\pm0.09_C$	95.3	$6.13\pm0.53_F$	$2.43\pm0.02_Z$	99.3

Table 1. Modeling drying kinetics of orange peel using diffusion models. Subscripts (A,B,C); (D,E,F); (X,Y,Z) show homogenous groups established from LSD intervals ($p<0.05$).